JOURNAL OF BACTERIOLOGY, Sept. 1985, p. 1172–1179
0021-9193/85/091172-08$02.00/0

Vol. 163, No. 3

Regulation of Single and Multicopy *his* Operons in *Escherichia coli*

ANDREA RICCIO,[1,2] CARMELO B. BRUNI,[2] MARTIN ROSENBERG,[3]† MAX GOTTESMAN,[4] KEITH McKENNEY,[3]‡ AND FRANCESCO BLASI[1]*

International Institute of Genetics and Biophysics, CNR, Naples, Italy[1]; Centro di Endocrinologia e Oncologia Sperimentale, CNR, Naples, Italy[2]; and Laboratory of Biochemistry[3] and Laboratory of Molecular Biology,[4] National Cancer Institute, Bethesda, Maryland 20205

Received 25 February 1985/Accepted 13 May 1985

We fused segments of the *Escherichia coli his* regulatory region to *galK* in single-copy and multicopy vectors. These fusions demonstrated that (i) derepression of *his* by histidine starvation is due exclusively to attenuation; (ii) the *his* promoter is metabolically regulated; and (iii) both regulatory systems operate when the *his* regulatory region is present on a multicopy plasmid. Thus, there is no evidence for titration of *his* regulatory elements. Deletions of the *his* anti-attenuator region, carried on multicopy plasmids, cause low-level *galK* expression. This expression is not stimulated by histidine starvation, but is growth rate dependent. We replaced the *his* attenuator with the efficient lambda terminator, t_o. In the context of the *his* regulatory region, however, λt_o only partially terminates transcription.

The expression of the *his* operon of *Escherichia coli* is regulated by histidine-specific attenuation at a rho-independent transcription termination site preceding the first structural gene (5, 12). RNA polymerase initiating from the *hisGp* promoter may terminate at this site, producing a 181-nucleotide leader RNA (9, 25), or may proceed beyond the attenuator into the *his* structural genes. The nucleotide sequence of the *his* leader RNA allows two alternative secondary structures. One structure contains at the 3′ end a hairpin, followed by a run of uridylate residues; this is the attenuator configuration and the site of transcription termination. When the competing structure forms, termination is prevented, and *his* is transcribed. The secondary structure of the leader RNA is dictated by the translation rate of a sequence rich in histidine codons, present at the 5′ end of the leader RNA, where ribosomes may pause or stall when the concentration of histidyl tRNA becomes limiting (5, 12).

We studied *his* regulation by cloning DNA fragments containing the promoter region or attenuator region or both into plasmid pKO1 (18) and assaying the transcriptional properties of these fragments in vivo and in vitro. The responses of the clones to histidine-specific and growth rate-dependent signals were analyzed in both multiple and single copies. The system was further exploited to generate substitutions and deletions within the leader RNA region to dissect the phenotype of *his* leader RNA deletions and to demonstrate that sequence context can affect the efficiency of transcription termination.

MATERIALS AND METHODS

Media, growth conditions, and enzyme assays. LB medium and M59 minimal medium (16) supplemented with 0.5% glucose were used routinely. Solid media contained 1.5% agar. When necessary, L-proline (1 mM), thiamine (10 μg/ml), ampicillin (50 μg/ml), or tetracycline (10 μg/ml) was added. Histidine limitation was obtained by adding 3-amino-1,2,4-triazole (4) to logarithmically growing cells in the presence of 0.4 mM adenine. Galactokinase assays were carried out by using cells grown to an A_{650} of 0.5 and a previously described procedure (18).

Materials. ^{14}C-labeled D-galactose (60 mCi/mmol), [α-^{32}P]CTP (400 Ci/mmol), and [^{14}C]UTP (400 Ci/mmol) were obtained from Amersham Corp., Arlington Heights, Ill. Restriction endonucleases and T4 DNA ligase were obtained from New England Biolabs, Waltham, Mass. T4 polynucleotide kinase and alkaline phosphatase from calf intestine were purchased from Boehringer Mannheim Biochemicals, Indianapolis, Ind. *E. coli* RNA polymerase was obtained from Miles Laboratories, Inc., Elkhart, Ind. Mung bean nuclease was obtained from P-L Biochemicals, Inc., Milwaukee, Wis.

***E. coli* strains, plasmids, and phages.** *E. coli* K-12 strains N100 (*galK2 recA13 pro sup thi*), N113 (N100 lysogenic for λ *imm*^{434}), and S165 Δ(*galETK*) were used. Multicopy plasmids pKO1, pKO4, and pKG1800 have been described previously (18). Plasmids pAR1 and pAR3 were constructed by cloning different *Alu*I fragments of the *his* regulatory region from plasmid pCB3 (5) into the single *Sma*I site of pKO1 (Fig. 1 and 2). pAR6 was constructed by cloning the *Hin*dIII-*Bgl*II fragment of pAR1 (containing the *hisGp* promoter) into *Hin*dIII- and *Bam*HI-cut pKO4, a derivative of pKO1 containing single *Hin*dIII and *Bam*HI sites. Plasmid pARX was obtained in two steps (Fig. 2B). First, a 190-base pair *Sau*3A fragment of bacteriophage λ containing the λt_o terminator (22, 23) was inserted into the single *Bgl*II site of pAR1. A *Hin*dIII-*Hin*cII fragment from a recombinant containing the λt_o terminator in the correct orientation (pAR7) was isolated. This fragment, containing the *hisGp* promoter followed by the λt_o terminator, was inserted into pKO1, which had been cut with *Hin*dIII and *Sma*I. All of these constructions except pARX were verified by restriction analysis; in pARX the insertion was sequenced.

Phage λ derivatives of plasmids pAR1 and pAR6 were obtained by a modification of a technique described previously (18). Strain N100 carrying pAR1 and pAR6 plasmid

* Corresponding author.
† Present address: Department of Molecular Genetics, Smith Kline & French Laboratories, Swedeland, PA 19479.
‡ Present address: Laboratory of Molecular Genetics, National Institute of Neurological and Communicative Disorders and Stroke, Bethesda, MD 20205.

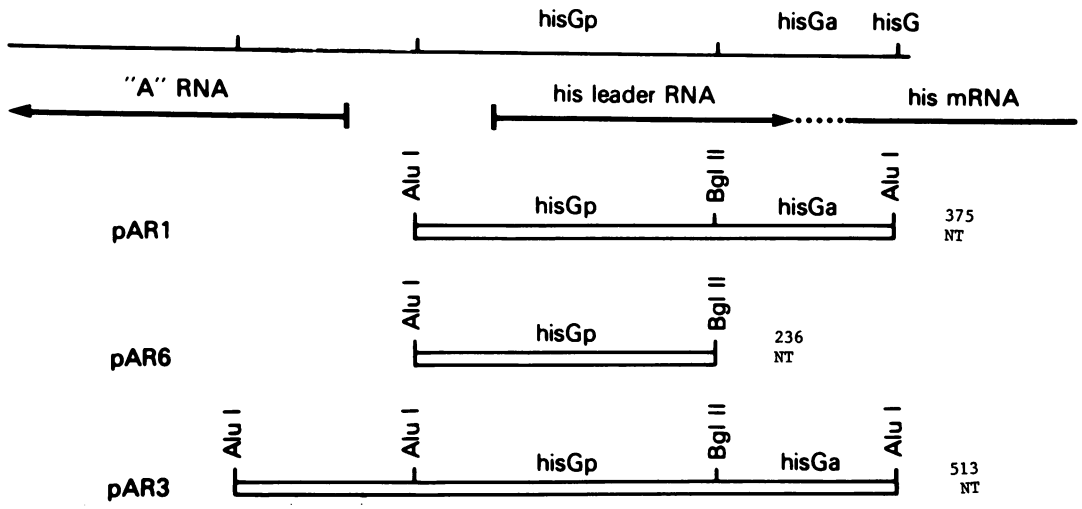

FIG. 1. Genetic and restriction map of the *E. coli his* regulatory region. The top line shows the *his* promoter (*hisGp*), the *his* attenuator (*hisGa*), and the beginning of the first *his* structural gene (*hisG*). The second line indicates the transcription pattern of this region. Rightward transcription initiating at *hisGp* may or may not terminate at *hisGa* (dotted line). A leftward transcript ("A RNA") of unknown function is also shown. The three open bars at the bottom represent the *his* DNA restriction fragments used in this work; the names of the pKO1 derivates containing these fragments are indicated. NT, Nucleotides.

DNA was infected with λ *c*I857 *gal-8*, and recombinant phages were selected at 32°C by plating the lysate on strain S165, using tryptone tetrazolium-galactose agar plates. The majority of the plaques appeared red on the galactose indicator plates, but 0.2% had a clear phenotype. The latter were produced by phage that had lost *galET* but retained *galK* and the recombinant *his* regions from pAR1 or pAR6. They had the following structure: (λ *b-galK-his-attL*). In the absence of galactose these phage gave cocarde-shaped plaques. A DNA restriction enzyme analysis of the purified phage confirmed their recombinant structure. Single-copy lysogens of pAR1 and pAR6 in strain S165 were obtained by infection and were maintained at 32°C.

In vitro transcription. Supercoiled plasmid DNA was transcribed in vitro as described previously (9). RNA polymerase (100 to 200 μg/ml), DNA (20 to 30 μg/ml), KCl (100 mM), heparin (100 μg/ml), and nucleotide triphosphates (at concentrations of 0.2 mM, except ^{32}P-labeled CTP and UTP, which were used at concentrations of 0.04 mM) were incubated for 30 min in 20 mM Tris (pH 7.9) at 37°C. The mixture was extracted with phenol and analyzed by electrophoresis on 6% polyacrylamide gels in 7 M urea.

Determination of plasmid copy number. We used a dot blot hybridization technique in which different amounts of bacterial cultures were spotted onto nitrocellulose paper (A. B. Chepelinsky and M. Rosenberg, submitted for publication). The filter was treated as described previously for the colony hybridization procedure (16) and was hybridized to an excess of ^{32}P-labeled pBR322 (1 μg). Appropriate DNA standards were used. The filter was exposed to X-ray films, and the intensities of the spots were quantitated by densitometric scanning.

DNA sequencing. The technique of Maxam and Gilbert (17) was used for DNA sequencing.

In vitro deletions. Short deletions at the *Bgl*II site of pAR1 (see below) were obtained by digesting *Bgl*II-linearized plasmid DNA with mung bean nuclease. A 20-μg portion of linearized plasmid DNA was incubated with 135 U of mung bean nuclease at 30°C for 30 min in a 400-μl reaction mixture containing 0.03 M sodium acetate buffer (pH 5.6), 0.250 M NaCl, 1 mM ZnCl, and 5% glycerol. The mixture was then extracted with phenol, precipitated with ethanol, incubated with T4 DNA ligase (16), and digested with *Bgl*II. The final mixture was used to transform strain N100. Transformations were carried out as previously described (6). Selection and analysis of *his* leader deletions are described below.

RESULTS

Fusion of the *his* regulatory region to the *galK* gene: histidine-specific regulation. Different fragments of the *E. coli* K-12 *his* operon regulatory region were cloned in plasmid pKO1, a vector system specifically devised to study transcription regulatory signals (18). Plasmid pKO1 is a derivative of pBR322 carrying the *E. coli galK* gene without its cognate promoter. When a promoter is inserted upstream from *galK*, pKO1 can complement a GalK$^-$ host.

Figure 1 shows a restriction map of a 700-base pair region encompassing (from right to left) the 5′ end of the *hisG* gene, the *hisGa* attenuator, and the *hisGp* promoter (9, 25). The different fragments relevant to the present study are also indicated in Fig. 1. The details of plasmid construction are described above; plasmid structures are shown in Fig. 2. Plasmids pAR1 and pAR3 carry the entire *his* regulatory region, including the promoter and attenuator; pAR3 contains an additional 138 base pairs located at the 5′ end of the *hisGp* promoter (Fig. 1 and 2A). Plasmid pAR6 is identical to pAR1 except for deletion of the *hisGa* attenuator. This multicopy plasmid system allowed us to answer the following questions: (i) What is the minimum *his* region required for regulation? (ii) Are *his* attenuation and promoter regulation separable? (iii) Is *his* regulation maintained when the *his* regulatory elements are present in high copy number?

We tested the response of each of the plasmids described above to the intracellular histidine concentration. Histidine limitation is known to cause derepression of the *his* operon (4). Table 1 shows that pAR1 showed eightfold induction when histidine limitation was induced by treatment with 20 mM aminotriazole for 8 h. This value agrees well with measurements of *his* enzyme levels (4). Lower specific activity was obtained when we used a lower concentration of

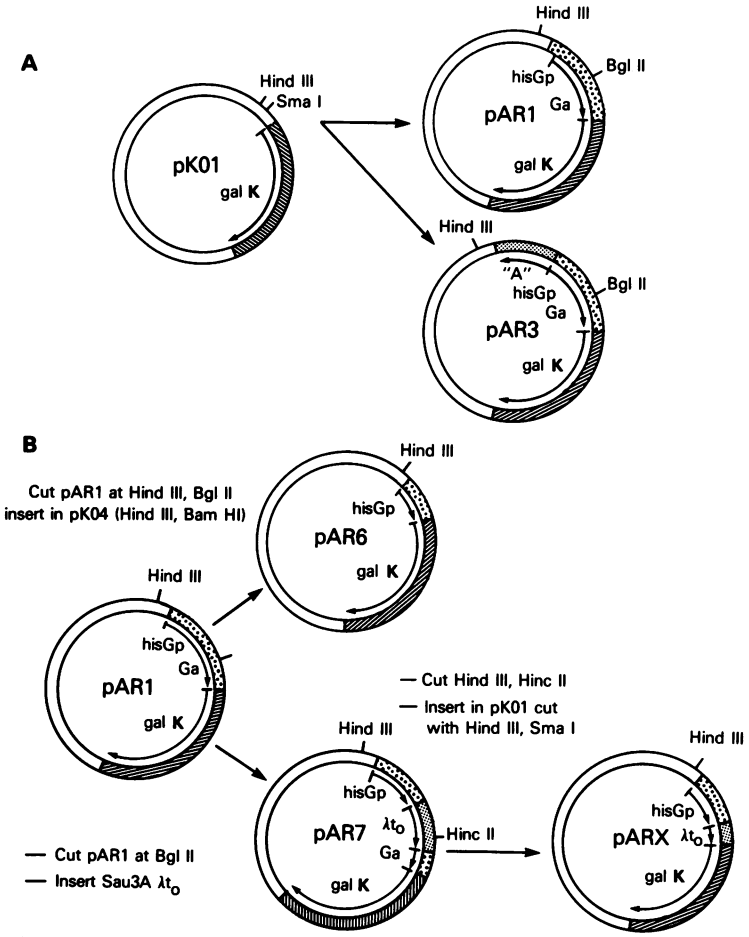

FIG. 2. Construction of plasmids. (A) Plasmids pAR1 and pAR3 carrying *hisGp* and *hisGa* were constructed by inserting the appropriate *Alu*I fragment (see Fig. 1) into *Sma*I-linearized pKO1. (B) Derivatives of pAR1: pAR6 (deleted for *hisGa*), pAR7 (an insertion of λt_o), and pARX (a substitution of λt_o for *hisGa*). The initiator triplet AUG of the leader peptide is at position 32; the terminator triplet is at position 80.

aminotriazole (4 mM) and a shorter exposure to the inhibitor (2 h). A similar derepression ratio was obtained with plasmid pAR3, which contains an additional 259 base pairs of *his* region DNA 5′ to the *his* leader RNA start (Table 1). A *galEp-galK* fusion (pKG1800) showed no response to histidine limitation. From these results it appears that the fragment cloned in pAR1 carries the necessary *his* control elements and that *his* regulation may be as faithful in high copy number as it is in a single *his* operon copy.

Deletion of the *his* attenuator (pAR6) resulted in a threefold increase in galactokinase levels under repressed conditions (Table 1). In contrast to plasmids pAR1 and pAR3, no increase was observed under histidine-limiting conditions (Table 1). The galactokinase levels of pAR6 were significantly lower than those of derepressed pAR1. This difference can be accounted for by the lower copy number of pAR6. Correction for copy number brought the galactokinase levels of pAR6 to the levels of derepressed pAR1 (Table 1). We conclude that histidine regulates the *his* operon entirely by an attenuation mechanism.

To confirm the conclusions described above, we transferred the pAR1 and pAR6 recombinant *his* fragments onto a λ*galK* phage, lysogenized an *E. coli galK* strain, and measured the effect of histidine limitation on the expression of the now single copies of *hisGp-galK* operon fusions. A 15-fold increase in galactokinase activity was observed when λAR1 lysogens were subjected to histidine limitation by adding aminotriazole to the medium (Table 2). The derepressed levels of galactokinase were about 40-fold lower than the levels in multicopy plasmid pAR1 under derepressing conditions (Table 1), in accord with the copy numbers of these pBR322-based plasmids. The expression of galactokinase from λAR6 was identical under repressed and derepressed conditions and was comparable to that of derepressed λAR1.

Growth rate-dependent (metabolic) regulation at the *his* promoter. In addition to histidine-specific regulation, the *his* operon is also subject to metabolic growth rate-dependent regulation, which is mediated by ppGpp (24, 26). The level of histidine enzymes decreases when cells are grown in rich media. We analyzed the responses of plasmids pAR1, pAR3, and pAR6 to variations in the growth rate by growing cells in different media and assaying their galactokinase levels. In all of the strains tested, the highest levels of *galK* expression were obtained with slowly growing cells (minimal medium) whether the plasmids contained the *hisGa* attenuator or not (Table 3). As expected, no evidence of growth rate regulation was observed when *galK* was driven by the *galEp* promoter (pKG1800). Growth rate regulation was also observed with the single-copy fusions (data not shown). These

TABLE 1. Histidine-specific regulation of galactokinase levels in *E. coli galK* strains carrying recombinant *his-galK* fusion plasmids

Plasmid	Sequence cloned before *galK*	Galactokinase level[a]		Relative plasmid copy no.		Corrected galactokinase level[b]	
		R assay	D assay	R assay	D assay	R assay	D assay
pAR1	*hisGp hisGa*	200	1,606	1.0	1.0	200	1,606
pAR6	*hisGp*	561	476	0.22	0.25	2,550	1,904
pKG1800	*galEp*	416	307	1.0	0.9	416	338
pAR3	*hisGp hisGa*	232	1,713	1.1	1.04	210	1,700

[a] See reference 18. R and D assays were performed with cells grown in minimal medium and with cells grown in the presence of 20 mM aminotriazole for 8 h, respectively.
[b] Galactokinase level divided by the relative plasmid copy number.

results agree with previous observations which showed that metabolic regulation is attenuator independent and hence is likely to result from control of promoter activity (24, 26). The 14-fold difference which we observed with the plasmid system is close to the 10-fold difference reported by other workers for the chromosomal operon. These results show that metabolic regulation is still maintained when the *his* promoter region is present in high copy number.

In vitro generation of leader RNA deletion mutants. The pKO1 system may be used to select mutations in the regulatory elements cloned upstream from *galK* (20). Plasmid pAR1 contains a unique *Bgl*II site within the *his* regulatory region, which is located within the loop of the C-D hairpin structure (Fig. 3, nucleotide 115). This site lies in a critical position between the C-D loop and the descending D-stem region. The D stem is thought to participate in the alternative D-E antiterminator structure which prevents the formation of the E-F attenuator (5, 12). In *Salmonella*, small deletions in the C-D stem-loop produce a His^- phenotype; the decreased probability of forming an efficient D-E antiterminator stem-loop leads to a leader RNA structure that is frozen in the attenuator configuration (12). However, our multicopy system might permit a finer assessment of the degree of attenuation in these mutants. Therefore, we generated deletions of the corresponding region of the *E. coli his* leader, digesting *Bgl*II-linearized pAR1 DNA with mung bean nuclease, religating, transforming strain N100 (*galK*$^-$), and selecting ampicillin-resistant colonies on MacConkey-galactose indicator plates. The pKO1 system detects strains with plasmids that express *galK* (red) colonies among Gal^- (white) colonies. In our experiment 95% of the transformants displayed a Gal^+ phenotype, and 5% displayed a Gal^- phenotype. Colonies of both types were isolated for analysis. Deletion mutants (pAR8) were identified by isolating DNAs from several Amp^r transformants, digesting these DNAs with *Bgl*II and *Hae*III, and determining the size of the deletion by polyacrylamide gel electrophoresis. Plasmids pAR8-R1, pAR8-R2, and pAR8-W3 were shown to have lost the *Bgl*II site and, by subsequent DNA sequence analysis, to carry deletions of 4 (*hisL*115-118), 8 (*hisL*111-118), and 20 (*hisL*103-122) nucleotides, respectively. The structures of these three mutants are shown in Fig. 3, and their phenotypes are summarized in Table 4. We found that the expression of galactokinase was inversely related to the extent of the deletion, but that each mutant yielded detectable galactokinase activity. The largest deletion mutant, pAR8-W3, which was Gal^- on MacConkey-galactose indicator plates, still showed ~20% of pAR1 galactokinase activity (Table 4). In contrast to the behavior of wild-type pAR1, plasmids pAR8-R1, pAR8-R2, and pAR8-W3 were not derepressed by aminotriazole.

TABLE 2. Galactokinase levels in single-copy λ *hisGp-galK* lysogens

Phage	Promoter	Attenuator	Galactokinase level[a]	
			R assay	D assay
λAR1	*hisGp*	*hisGa*	2.4	39.5
λAR6	*hisGp*	None	30.2	32.1

[a] See Table 1, footnote *a*.

TABLE 3. Growth rate-dependent regulation of the *his* promoter on multicopy plasmids

Plasmid	Galactokinase level[a]		
	M56 medium	M56 medium + Casamino Acids	LB medium
pAR1	270	147	80
pAR6	1,909	1,003	137
pAR3	290	NT[b]	79

[a] See Table 1, footnote *a*. Galactokinase levels wre normalized to the plasmid copy number of pAR1.
[b] NT, Not tested.

Although the three mutants could not be derepressed, they were subject to metabolic regulation. All showed substantially more *galK* expression in M56 medium than in LB medium (Table 4).

Substitution of a λ terminator for the *hisGa* attenuator. The regulation of transcription termination at the *hisGa* attenuator depends upon histidine-controlled competition between alternative RNA duplexes. Partial deletion of the antiterminating structure increases attenuation (12). Analogously, replacement of the attenuator with a terminator without homology to the *his* leader should have the same effect (viz., little readthrough transcription should be observed). We tested this prediction by substituting the t_o terminator of bacteriophage λ for the *hisGa* attenuator, taking advantage of the *Bgl*II site that separates the *hisGp* promoter from the *hisGa* attenuator in pAR1 (Fig. 2B) (see above). The resulting plasmid, pARX (Fig. 2B), carries *galK* downstream from a regulatory region composed of the *hisGp* promoter, the *his* leader region up to the *Bgl*II site, and the λt_o terminator. The sequence of this portion of the plasmid, along with a possible RNA secondary structure, is shown in Fig. 4.

Two kinds of experiments were performed to test the effect of the λt_o terminator on transcription initiated at *hisGp*. First, galactokinase activity was measured in strain N100(pARX) and compared with the galactokinase activities of control strains carrying pAR1, pAR6, pAR7, or pAR52 (Table 5). Plasmid pAR52, which contains the *galEp* promoter upstream from λt_o and *galK*, did not synthesize galactokinase. This is consistent with previous in vitro demonstrations that the λt_o terminator is highly efficient both in its original genetic location (10) and in hybrid constructions when it is inserted between the *galEp* (20) or *lacZp* (McKenney, manuscript in preparation) promoters and *galK*. In contrast, plasmid pARX displayed high galactokinase levels that were equivalent to 40% of the level of pAR6 (carrying *hisGp* and *galK* without an intervening

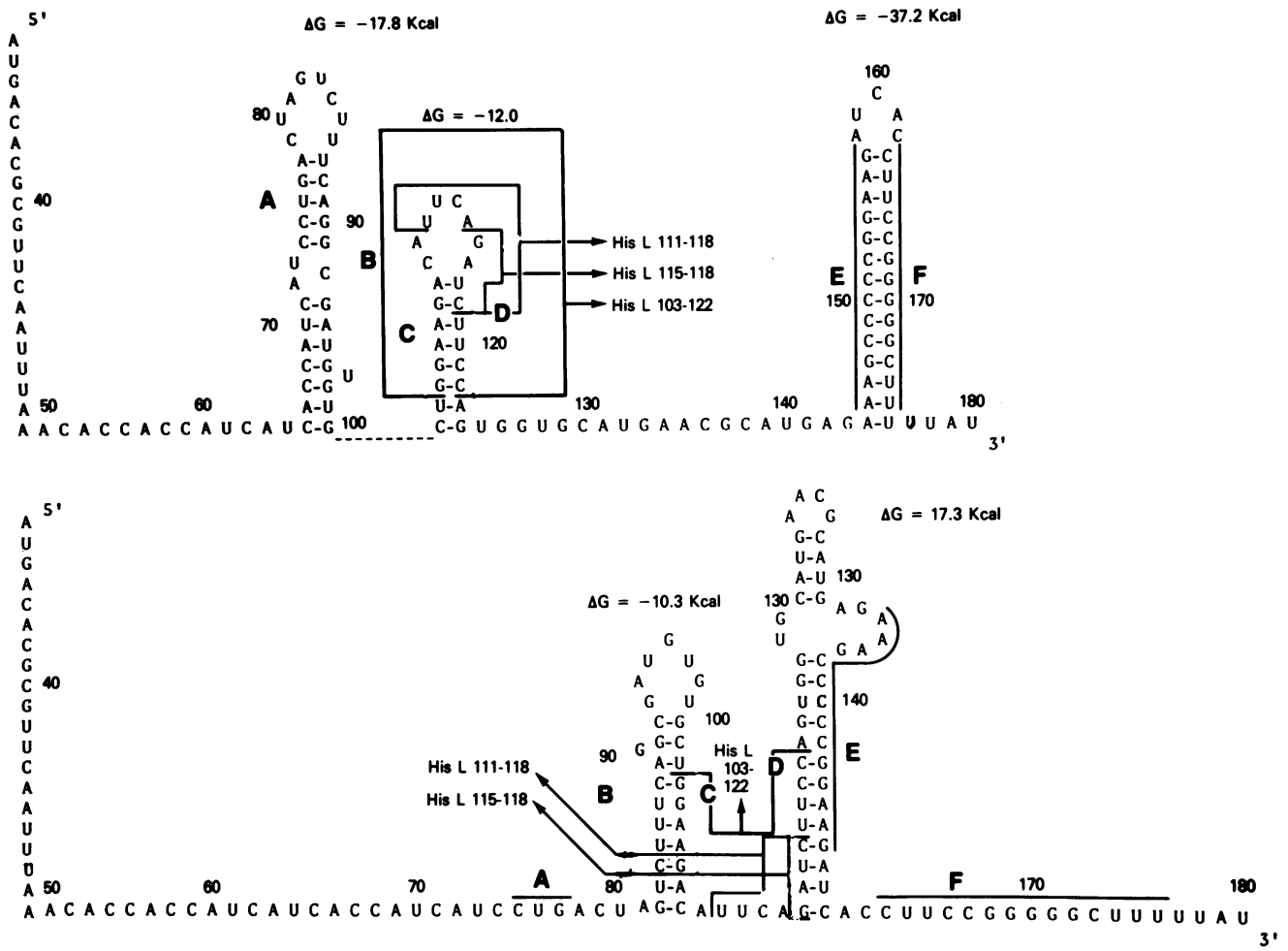

FIG. 3. Nucleotide sequence of three deletions around the *Bgl*II site (AGAUGU) of the *E. coli his* leader RNA. Sequences are arranged in a secondary structure leading to attenuation (top) or anti-attenuation (bottom), as visualized by Johnston and Roth (12) for the *S. typhimurium his* leader RNA.

attenuator). The expression of *galK* in strain N100(pARX) was independent of histidine regulation, since it was not augmented with aminotriazole treatment. Finally, the failure of *hisGp*-initiated transcription to terminate at λt_0 was not epistatic to *hisGa*; pAR7, which carries the sequence *hisGp*, λt_0, *hisGa*, and *galK*, does not synthesize galactokinase.

Our data show that the efficiency of the λt_0 terminator is context influenced; it can be nearly 100% effective in several different locations, but is only weakly active when it is cloned into the *his* leader region.

A second set of experiments excluded the possibility that *galK* expression in pARX was due to a new promoter created fortuitously between λt_0 and *galK* during the construction of the plasmid. DNAs from plasmids pAR1, pARX, and pAR7 (with structures *hisGp-hisGa-galK*, *hisGp*-λt_0-*galK*, and *hisGp*-λt_0-*hisGa-galK*, respectively [Fig. 2B]) were transcribed in vitro. After incubation of supercoiled DNA with purified RNA polymerase in the presence of [^{32}P]UTP, the RNA products were isolated and analyzed by polyacrylamide gel electrophoresis. Figure 5 shows the results of this experiment. Control plasmid pAR1 (Fig. 5, lanes A) produced the expected 181-nucleotide *his* leader RNA (9). In plasmids pARX and pAR7, transcription initiating at *hisGp* and terminating at λt_0 yielded a 190-nucleotide RNA (Fig. 4). Transcripts of pARX that read through λt_0 would not have been detected under our experimental conditions. However, plasmid pAR7, which has two transcription terminators in tandem, showed two discrete bands (Fig. 5, lanes B). The 190-nucleotide band represents transcription terminating at λt_0, whereas the 370-nucleotide band indicates transcripts reading through λt_0 and terminating at *hisGa*. For either template, the intensity of the 190-nucleotide band reveals that λt_0 is only 11 to 16% efficient (Table 6) in the *his* leader context, a value consistent with in vivo measurements. Thus, the expression of *galK* in pARX can be accounted for by readthrough of λt_0, rather than by a new promoter created during plasmid construction.

DISCUSSION

In this study we analyzed the regulation of the *E. coli his* operon by using several *his-galK* operon fusions. Our results support the mechanisms of *his* control that were proposed on the basis of *his* enzyme assays. However, the behavior of some of our constructions is not readily explained by existing models.

The *his* operons of *E. coli* and *Salmonella typhimurium*

TABLE 4. Properties of deletion mutants of the *his* leader RNA region

Plasmid[a]	Deletion[b]	Phenotype on MacConkey-galactose agar plates	Galactokinase level[c]		
			LB medium	M56 medium	M56 medium + 4 mM aminotriazole
pAR1	None	GalK$^+$ (red)	74	241	718
pAR8-R1	Nucleotides 115-118	GalK$^+$ (red)	85	190	205
pAR8-R2	Nucleotides 111-118	GalK$^+$ (red)	58	120	130
pAR8-W3	Nucleotides 103-122	GalK$^-$ (white)	15	47	44

[a] Plasmids were used to transform *E. coli* K-12 *galK* strain N100, which forms white colonies on MacConkey-galactose agar plates.

[b] Deletions of the *his* leader RNA region. Nucleotides in this region are numbered by starting with the transcription initiation site of the *his* operon as nucleotide 1 (9, 12).

[c] See Table 1, footnote *b*. Derepression experiments were performed with 4 mM aminotriazole for 4 h. Under these conditions derepression levels lower than those shown in Table 1 (20 aminotriazole mM for 8 h) were obtained.

respond to the levels of charged histidyl tRNA, which in turn reflect the concentration of intracellular histidine (15). This regulation occurs by attenuation of transcription at *hisGa*, a stem-loop structure between the *his* promoter (*hisGp*) and *hisG* (5, 7, 8, 12, 13). When *his* tRNA levels are high, 95% of the transcripts initiating at *hisGp* terminate at *hisGa*, forming a 181-nucleotide leader RNA. If *his* tRNA is limiting, slow translation of *his* codons in the *his* leader leads to transcrip-

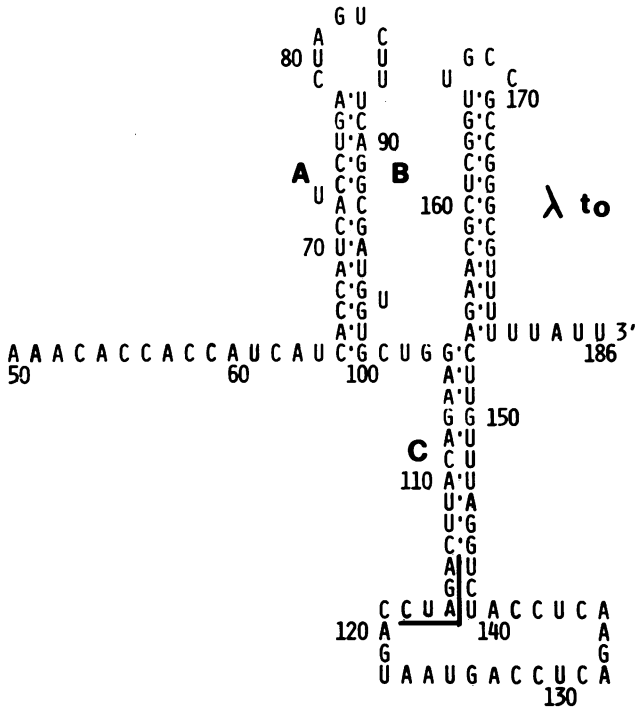

FIG. 4. Nucleotide sequence and putative secondary structure of the hybrid *his*-λt_o RNA. The underlined pentanucleotide AGAUC represents the *Bgl*II-*Sau*3a *his*-λt_o junction. A, B, and C indicate the *his* leader RNA sequence shown in Fig. 3.

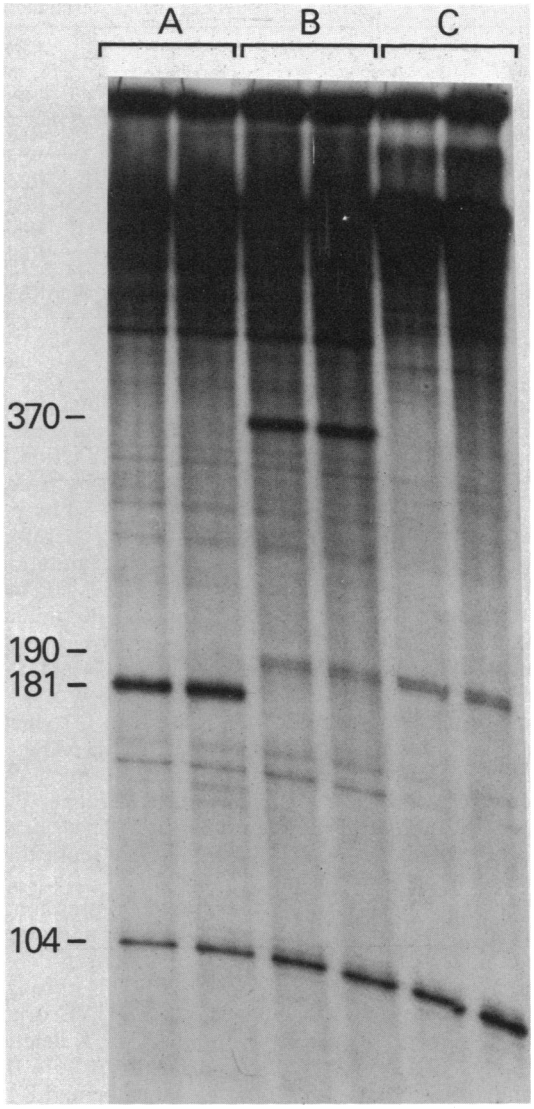

FIG. 5. In vitro transcription of supercoiled plasmid templates pAR1 (lanes A), pAR7 (lanes B), and pARX (lanes C). The two lanes for each plasmid represent duplicate transcription experiments. The conditions used are described in the text. A *Hae*III digest of φX174 was used as a marker to estimate the size of the 370-nucleotide band. The size of the 181-nucleotide band was determined by nucleotide sequence (9), as was the size of the 104-nucleotide band (14). The size of the 190-nucleotide band was estimated by comparing its migration with that of the 104-, 181-, and 370-nucleotide bands.

tion readthrough into the *his* structural genes. The presence of ribosomes on the *his* leader RNA is thought to favor the formation of an RNA structure that competes with *hisGa*.

The *his* operon is also metabolically regulated; *hisGp* is stimulated by ppGpp and is thus more active in cells growing slowly in minimal medium. This control is independent of the attenuator mechanism (2, 4, 26).

Cloned fragments of the *his* regulatory region. A 375-base pair *E. coli his* fragment, composed of *hisGp*, the *his* leader, and *hisGa*, appears to contain all of the *cis* elements required for *his* regulation. An operon fusion of this fragment to *galK* is 10-fold derepressed by aminotriazole, an inhibitor of histidine biosynthesis. The same derepression ratio is ob-

TABLE 5. Effect of the λt_o terminator on *galK* expression from the *galEp* and *hisGp* promoters

Plasmid	Promoter	Terminator	Phenotype on MacConkey-galactose plates	Galactokinase level[a]		
				M56 medium + Casamino Acids	M56 medium	M56 medium + aminotriazole
pKG100	*galEp*	None	Red	400	390	500
pAR52	*galEp*	λt_o	White	15	ND[b]	ND
pAR1	*hisGp*	*hisGa*	Red	104	241	718
pARX	*hisGp*	λt_o	Red	ND	868	785
pAR7	*hisGp*	λt_o *hisGA*	White	ND	ND	ND
pAR6	*hisGp*	None	Red	ND	2,119	2,224

[a] Values were normalized to the plasmid copy number of pAR1. Derepression was performed with 4 mM aminotriazole for 4 h (see Table 4, footnote *c*).
[b] ND, Not detectable.

served whether the fusion is present on a multicopy plasmid (pAR1) or in a single-copy λ prophage. This argues against the existence of a limiting *his* regulatory function, either positive or negative, which might be titrated by pAR1.

The induced level of galactokinase expressed by pAR1 is close to that of pAR6, which lacks *hisGa*. Therefore, the suppression of the attenuator during histidine limitation must be almost complete. As expected, *galK* expression in pAR6 is independent of histidine concentration. Plasmids pAR6 and pAR1 are growth rate regulated; galactokinase levels are highest in minimal medium, intermediate in Casamino Acids enriched minimal medium, and lowest in LB broth.

The presence of *hisGp* in pAR6 leads to a reduction in plasmid copy number; this is not the case in pAR1, where *hisGa* blocks readthrough into pBR322 sequences. The efficiency of *hisGp* is high, about fourfold higher than the efficiency of the *galEp* promoter (Table 1). That very active promoters cloned into pBR322 inhibit its replication has been reported previously (1).

Deletions of the D-E anti-attenuator. Derepression of the *his* operon depends on the formation of the anti-attenuator D-E structure (Fig. 4). We have generated *E. coli hisL* deletions of nucleotides 115 through 118, 111 through 118, and 103 through 122 which affect the C-D or D-E structures. These are similar to the *S. typhimurium hisL* deletions of nucleotides 109 through 119, 110 through 118, 116 through 120, and 116 through 124 isolated by Johnston and Roth (11, 12). The *S. typhimurium* mutants displayed a His^-, aminotriazole-sensitive phenotype (i.e., very low and nonducible expression of *his* enzymes). Our deletions, when present on a multicopy plasmid, show a more complex phenotype. In agreement with the single-copy analysis, *galK* expression in deletion plasmids pAR8-R1, pAR8-R2, and pAR8-W3 is not increased by aminotriazole. However, the basal level of *galK* expression ranges from 20% of wild-type levels for the largest deletion up to 80% for the smallest. Additionally, all of the deletions completely eliminate the ability of ribosomes to influence the equilibrium between the attenuator and anti-attenuator structures. The *his* leader RNA resembles in its secondary structure histidyl tRNA and may interact with histidyl RNA synthetase or *hisG* product (3). Our deletions include the anticodon-like sequences of the leader transcript. Therefore, it is possible that interactions between these sequences and other factors are required for full *his* attenuation. Of course, the precise role of the deleted nucleotides is unknown; isolation of appropriate point mutations will be required to extend this study.

Whether the *S. typhimurium* C-D deletion mutations would display a low-level constitutive phenotype if they were cloned onto a multicopy plasmid is not yet known.

Substitution of the λt_o terminator for *hisGa*. In its own context or cloned downstream from the *galp* and *lacp* promoters, the λt_o terminator is more than 95% efficient in vivo (Table 5) (20). In contrast, when placed in the *his* leader sequence at the *hisGa* site, it is only about 15% efficient in vitro or 60% efficient in vivo. The efficiency of cloned λt_o is not affected by histidine concentration.

The position effect on the activity of λt_o might be due to several causes. Although a sequence search of the *his* leader RNA did not reveal homologies with λt_o, competing secondary structures cannot be entirely ruled out a priori. It is known that the efficiency of terminators can be affected by nearby translation (2, 21). Although the activity of λt_o was not affected by aminotriazole, it might nevertheless be reduced by translation of the *his* leader. We have not yet tested this hypothesis. Finally, λt_o is in part dependent on transcription termination factor rho (10). The ability of rho to promote termination is influenced strongly by the length and sequence of the RNA upstream to the terminator. In particular, terminators distal to regions of potential secondary

TABLE 6. Efficiency of transcription termination of the *hisGp*-initiated transcripts at the λt_o terminator

Plasmid	Efficiency of transcription termination[a]				% Termination at λt_o	% Termination at *hisGa*
	104-Nucleotide RNA	181-Nucleotide *his* leader RNA	190-Nucleotide *his* λt_o hybrid leader RNA	370-Nucleotide *his* λt_o *hisGa* hybrid leader RNA		
pAR1	100	240				100
pAR7	100		70	360	16[b]	84[b]
pARX	100		35		NM[c]	

[a] The data were normalized by dividing the amount of [^{32}P]UMP incorporated in individual bands by the amount of [^{32}P]UMP in the 104-nucleotide RNA (14).
[b] Termination was calculated by assuming that the sum of the radioactivity in the 190- and 370-nucleotide bands equaled the total amount of the *hisGp*-initiated transcript, as it is for the 181-nucleotide band with the pAR1 DNA template (9).
[c] NM, Not measurable. The percentage of termination at λt_o could not be determined in the absence of a downstream terminator.

structure are poorly acted upon by rho (19). The highly structured *his* leader could block the access of rho to λt_o.

ACKNOWLEDGMENTS

F.B. and A.R. are very grateful to Maxine F. Singer for hospitality in her laboratory.

The part of this work carried out in Italy was supported by a grant from the Progetto Finalizzato Ingegneria Genetica Centro Nazionale delle Richerche to C.B.B. The Fogarty Center supported F.B. during his tenure at the National Institutes of Health.

LITERATURE CITED

1. **Adams, C. W., and G. W. Hatfield.** 1984. Effects of promoter strengths and growth conditions on copy number of transcription fusion vectors. J. Biol. Chem. **259**:7399–7403.
2. **Adhya, S., and M. Gottesman.** 1978. Control of transcription termination. Annu. Rev. Biochem. **47**:967–996.
3. **Ames, B. N., T. H. Tsang, M. Buck, and M. F. Christman.** 1983. The leader mRNA of the histine attenuator region resembles $tRNA^{His}$: possible general regulatory implications. Proc. Natl. Acad. Sci. U.S.A. **80**:5240–5242.
4. **Berberich, M. A., P. Venetianer, and R. F. Goldberger.** 1966. Alternative nodes of derepression of the histidine operon observed in *Salmonella typhimurium*. J. Biol. Chem. **241**:4426–4433.
5. **Blasi, F., and C. B. Bruni.** 1981. Regulation of the histidine operon: translation-controlled transcription termination (a mechanism common to several biosynthetic operons). Curr. Top. Cell. Regul. **19**:1–45.
6. **Dagert, N., and S. D. Ehrlich.** 1979. Prolonged incubation in calcium chloride improves the competence of *Escherichia coli* cells. Gene **6**:23–28.
7. **Di Nocera, P. P., F. Blasi, R. Di Lauro, R. Frunzio, and C. B. Bruni.** 1978. Nucleotide sequence of the attenuator region of the histidine operon of *Escherichia coli* K12. Proc. Natl. Acad. Sci. U.S.A. **75**:4276–4280.
8. **Ely, B., D. B. Fankhauser, and P. E. Hartman.** 1974. A fine structure map of the *Salmonella* histidine operator-promoter. Genetics **78**:607–631.
9. **Frunzio, R., C. B. Bruni, and F. Blasi.** 1981. In vivo and in vitro detection of the leader RNA of the histidine operon of *Escherichia coli* K12. Proc. Natl. Acad. Sci. U.S.A. **78**:2767–2771.
10. **Howard, B. H., B. de Crombrugghe, and N. Rosenberg.** 1977. Transcription *in vitro* of bacteriophage lambda 4S RNA: studies on termination and *rho* protein. Nucleic Acids Res. **4**:827–842.
11. **Johnston, H. M., and J. R. Roth.** 1980. Genetic analysis of the histidine operon control region of *Salmonella typhimurium*. J. Mol. Biol. **145**:713–734.
12. **Johnston, H. M., and J. R. Roth.** 1980. DNA sequence changes of mutations altering attenuation control of the histidine operon of *Salmonella typhimurium*. J. Mol. Biol. **145**:735–756.
13. **Kasai, T.** 1974. Regulation of the expression of the histidine operon in *Salmonella typhimurium*. Nature (London) **249**: 523–527.
14. **Levine, A. D., and W. D. Rupp.** 1978. Small RNA produced from the *in vitro* transcription of ColE1 DNA, p. 163–166. *In* D. Schlessinger (ed.), Microbiology—1978. American Society for Microbiology, Washington, D.C.
15. **Lewis, J. A., and B. N. Ames.** 1972. Histidine regulation in *Salmonella typhimurium*. XI. The percentage of transfer RNA His charged in vivo and its relation to the repression of the histidine operon. J. Mol. Biol. **66**:131–142.
16. **Maniatis, T., E. F. Fritsch, and J. Sambrook.** 1982. Molecular cloning: a laboratory manual. Cold Spring Harbor Laboratory, Cold Spring Harbor, N.Y.
17. **Maxam, A. M., and W. Gilbert.** 1980. Sequencing end-labeled DNA with base-specific chemical cleavages. Method Enzymol. **65**:499–560.
18. **McKenney, K., H. Shimatake, D. Court, U. Schmeissner, C. Brady, and M. Rosenberg.** 1981. A system to study promoter and terminator signals recognized by *Escherichia coli* RNA polymerase, p. 383–415. *In* J. G. Chirikjian and T. S. Papas (ed.), Gene amplification and analysis, vol. 2. Analysis of nucleic acids by enzymatic methods. North-Holland Publishing Co., Amsterdam.
19. **Morgan, W. D., D. G. Bear, and P. H. von Hippel.** 1984. Specificity of release by *Escherichia coli* transcription termination factor rho of nascent mRNA transcripts initiated at the lambda P_R promoter. J. Biol. Chem. **259**:8664–8671.
20. **Rosenberg, M., A. B. Chepelinsky, and K. McKenney.** 1983. Studying promoters and terminators by gene fusion. Science **222**:734–739.
21. **Rosenberg, M., and D. Court.** 1979. Regulatory sequences involved in the promotion and termination of RNA transcription. Annu. Rev. Genet. **13**:319–353.
22. **Sanger, F., A. R. Coulson, F. G. Hong, D. F. Hill, and G. B. Petersen.** 1982. Nucleotide sequence of bacteriophage lambda DNA. J. Mol. Biol. **162**:729–773.
23. **Schwarz, E., G. Scherer, G. Hobom, and H. Kossel.** 1978. Nucleotide sequence of cro, cII and part of the O gene in phage lambda DNA. Nature (London) **272**:410–414.
24. **Stephens, J. C., S. W. Artz, and B. N. Ames.** 1975. Guanosine-5′-diphosphate 3′-diphosphate (pp (Gpp)): positive effector for histidine operon transcription and general signal for amino-acid deficiency. Proc. Natl. Acad. Sci. U.S.A. **72**:4389–4393.
25. **Verde, P., R. Frunzio, P. P. Di Nocera, F. Blasi, and C. B. Bruni.** 1981. Identification, nucleotide sequence and expression of the regulatory region of the histidine operon of *Escherichia coli* K12. Nucleic Acids Res. **9**:2075–2086.
26. **Winkler, M. E., D. J. Roth, and P. E. Hartman.** 1978. Promoter- and attenuator-related metabolic regulation of the *Salmonella typhimurium*. J. Bacteriol. **133**:830–843.